Experimental and Analytical Behavior of HSC Columns Reinforced with Basalt FRP Bars

Abeer M. Erfan [a], Yasser A. Algash [b], Taha A. El-Sayed [c*]

[a,c] Department of Civil Engineering, Shoubra Faculty of Engineering, Benha University, 108 Shoubra St., Shoubra, Cairo, Egypt
[b] Aviation and Engineering Technology Institute, Structural Engineering Department, Cairo, Egypt

— — — — — — — — — ◆ — — — — — — — — —

ABSTRACT

This paper investigates the structural behavior of composite HSC columns reinforced longitudinally and transversely with BFRP bars under centrically axial loads. five full-scale concrete columns with a 200×200mm cross section and 2000mm in height were tested under axial monotonic loading. The Influence of the type of the reinforcement (steel and BFRP) and the concrete strength under concentric loading on the performance of the specimens was investigated. The samples were examined under concentric compressive load up to failure.
The results showed that the BFRP bar reinforced HSC (BFRP-HSC) specimens is as efficient as the steel bar reinforced HSC (steel-HSC) specimen in sustaining concentric axial load. The load–axial displacement, load–lateral displacement and failure mode of all the BFRP-reinforced HSC columns are presented and compared to that of the steel-reinforced HSC columns.
Also, a non-linear finite element analysis (NLFEA) using ANSYS Software ver. 14.5 was carried out to validate the behaviour of HSC-BFRP reinforced concrete columns under centric loads. The analytical results were agreed with the experimental results.

KEYWORDS: BFRP bars; Concrete column; Centric load; Deformation; Strength; Cracking; Ductility; Compressive behavior; confinement.

_____

- *Abeer M. Erfan , Lecturer, Egypt.*
  E-mail: abir.arfan@feng.bu.edu.eg
- *Yasser A. Algash, Egypt.*
  E-mail: dr_yaseralgash@yahoo.com
- **corresponding author: Taha A. El-Sayed, Associate Professor, Egypt.*
  E-mail: taha.ibrahim@feng.bu.edu.eg

1. INTRODUCTION

As of late, fiber-reinforced polymer (FRP) composites are accepting expanded consideration due to its predominant execution compared to customary steel [1]. A few exploratory and numerical thinks about explored the application of FRP composites as fortifying and reinforcing fabric for strengthened concrete (RC) structures [2–5]. In common, the execution of RC structures depends not as it were on mechanical characteristics of concrete and fortification but moreover on the composite activity between the two components [6,7]. This can be the case for any sort of fortification, counting FRP composite materials [8,9]. FRP bars had numerous preferences over steel bars, such as no erosion indeed in cruel chemical situations, a thickness of one-fifth to one-quarter of that of steel bars and great electromagnetic separator property. The utilize of FRP bars as elective fortifications in strengthened concrete was an inventive arrangement to overcome the erosion issue of the steel [10–12].

Basalt FRPs (BFRPs) have risen as a promising elective to routine FRPs in strengthening concrete structures [13]. BFRP has been demonstrated to appear beneficial characteristics in mechanical, chemical, working temperatures, and tall proportion of execution to taken a toll in comparison to other FRPs. So, Ibrahim et al. [14] proposed BFRP bars for application within the FSRC framework. Within the ponder of Ibrahim et al. [15], bond-slip behavior between BFRP bars and concrete was inspected through pull-out tests on 10-mm-diameter BFRP bars with five distinctive surface conditions. To speak to the neighborhood bond stress-slip relationship of the tried bars, Ibrahim et al. [15] appeared that the well-known BPE bond-slip show [16] can be connected.

By and by, extant studies on the application of FRPs to concrete structures basically center on the holding behavior between FRP bars and concrete [17–21] in conjunction with the flexural exhibitions of concrete individuals strengthened with FRP bars [22–27] and the mechanical properties of FRP-RC structures [28–32]. There's a lack of considers on the compression execution of FRP-RCCs and particularly on FRP-RCCs beneath offbeat loads. Subsequently, test considers on the mechanical properties of BFRP-RCCs are of awesome importance in growing the application of FRP bars in concrete structures.

BFRP has accumulated consideration as a substitution for other FRPs since of its cost-effectiveness, ease of fabricate, high-temperature resistance, freeze-thaw execution, great resistance to erosion, acids, and vibration and affect stacking [33-37]. Additionally, BFRP bars have way better strength in antacid conditions than AFRP and GFRP [35,38]. Due to these extraordinary highlights, there's an expanding application of BFRP bars in gracious designing structures. During the final few a long time, numerous endeavors have been made to examine the mechanical behavior of BFRP fortified concrete and steel strengthened geopolymer concrete auxiliary individuals counting pillars, columns, chunks and boards, in specific, the bond behavior between concrete and support, and by and large execution. The

flexural and shear execution of concrete pillars fortified with BFRP bars has been tentatively considered and displayed in Refs. [39-43], which appeared that concrete pillars strengthened with BFRP bars had higher qualities than control steel-reinforced bars with the same fortification proportion, and carried on very so also to that of bars fortified AFRP and GFRP bars.

This study aims to investigate the performance of using BFRP bars as longitudinal reinforcements on concrete columns and basalt stirrups when subjected to a centric load. For this purpose, five square RC columns with a cross-section of 200 mm X 200 mm and a height of 2000 mm were examined and tested till failure.

2. Experimental Study

The column specimens were examined under 5000kN universal testing machine The aim of this study was getting the ultimate failure load, ultimate mid span deflection, and failure mode for control column with respect to the others reinforced using basalt bars.

2.1. Material used

1. Fine aggregate: with 2.64 and 2.74 fineness modulus and specific gravity [44].
2. Coarse aggregate: with 2.89 specific gravity [44].
3. Cement: CEM I 42.5 N- Ordinary Portland with a specific gravity 3.15 [44].
4. Silica Fume: with 2.30 specific gravity.
5. Tapped Water: for mixing & curing.
6. Super plasticizer: 1.2kg/litre density [44].
7. Reinforcing steel: reinforcing normal mild steel 24/35 (plain bars) of diameter 6 mm & reinforcing high grade steel 36/52 (deformed bars) of diameter 10 and 12 mm [44].
8. Basalt fiber reinforced polymers (BFRP) bars; see Table 1 & Fig. 1.

Table 1: BFRP properties [43].

Property	Measured Value
Density (MPa)	2.68
Tensile Strength, f_u (MPa)	1400
Tensile Modulus (Gpa)	56
Ultimate Strain, ϵ_u (%)	24

Fig. 1. BFRP stirrups & Ribbed BFRP bars.

2.2. Experimental program and test setup

Five concrete columns having the cross section dimensions of 200 mm x200 mm with 2000 mm long were casted as indicated in Table 2. The concrete mix for the test specimens was designed to obtain compressive strength of 55MPa at 28days age. The mix proportions were 2 sand: 1 cement, water cement ratio was 0.35 and 2.0% super plasticizer by weight of cement. Two types of reinforcing bars were employed. All samples were examined under centric axial compression loadings. By using compression testing machine with capacity of 5000KN as shown in Fig. 2.b, the load was applied via loading cell which was acting at the column head. Incremental load was applied with an increment of 5 to 20KN for all the test specimens.
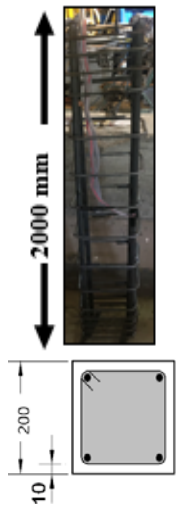

(a)   (b)   (c)

Fig.2: Experimental stages, a) Casting Columns; b) RFT. Basalt & Steel Cages c) Test Setup.

3. Test Results and Discussion

 The performance of the concrete columns reinforced with either steel reinforcement or BFRP basalt bars with different diameters and confined with different number of stirrups is presented and discussed below. The ultimate strength, lateral deflection and cracks pattern were investigated.

Table: 2 Details of tested concrete columns

Specimen Id.	Description	Reinforcing ratio μ(%)	RFT Configuration
Cs	Control specimen 200x200x2000 mm reinforced by 4Φ12 longitudinal steel bars and 12 Φ 8 steel stirrups	1.130	
C_{1-B12}	Concrete column reinforced using 4Φ12 longitudinal Basalt bars and 15 Φ 8 steel stirrups	1.130	
C_{2-B10}	Concrete column reinforced using 4Φ10 longitudinal Basalt bars and 15 Φ8 steel stirrup	0.785	
C_{3-B12}	Concrete column reinforced using 4Φ12 longitudinal Basalt bars and 10 Φ8 Basalt stirrup	1.130	
C_{4-B10}	Concrete column reinforced using 4Φ10 longitudinal Basalt bars and 10 Φ8 Basalt stirrup	0.785	

3.1 Experimental Ultimate load.

The the control specimen Cs was the control concrete column which reinforced with using 4Φ12 longitudinal steel bars and 7Φ 8/ m steel stirrups. The experimental failure load was 669.0 KN. For C_{1-B12} which reinforced using 4Φ12 basalt bars and 7Φ 8/ m steel stirrups, the failure load was 854.0 KN. This increase in failure load is due to the high tensile strength of basalt bars with an enhancement ratio 27.6%.

For column C_{2-B10} which use 4Φ10 longitudinal Basalt bars and 7Φ 8/ m steel stirrups, the experimental failure load was 739.0 KN with an enhancement ratio of 18.5 % due to the tension tensile strength of basalt bars.

For C_{3-B12} which reinforced using 4Φ12 basalt bars and 5Φ 8/ m steel stirrups, the failure load was 840.0 KN. This increase in failure load is due to the high tensile strength of basalt bars and good confinement of Basalt stirrups although its number is less than Cs in meter but it had high tensile strength with respect to steel.

The enhancement ratio in failure load is 25.5%. For C_{4-B10} which reinforced using 4Φ10

basalt bars and 5Φ 8/ m Basalt stirrups, the failure load was 720.0 KN with an enhancement ratio of 7.6% with respect to Cs.

According to the results in Table 3 the effect of using basalt reinforcement is so effective in increasing the failure load capacity especially in using basalt stirrups which impact in increasing the confinement of columns. The average enhancement ratio in case of using basalt bars or basalt bars and basalt stirrups is about 20.0% as shown in Table 3 & Fig. 3 to Fig. 5.

Table 3: Deformation of tested concrete columns

Specimen Id.	Exp. Failure Ld (KN)	Δ lateral P_{Umax} (mm)	Ductility (Δ 0.8 P_{Umax} / Δ P_{Umax})	Energy Absorption, KN.mm	% of Energy Absorption enhancement
Cs	669.0	4.25	1.15	1591.0	---
C_{1-B12}	854.0	5.30	1.07	2239.0	40.7
C_{2-B10}	739.0	4.50	1.13	1784.0	12.1
C_{3-B12}	840.0	5.10	1.08	2142.0	34.6
C_{4-B10}	720.0	4.10	1.07	1601.0	0.63
Average					22.0
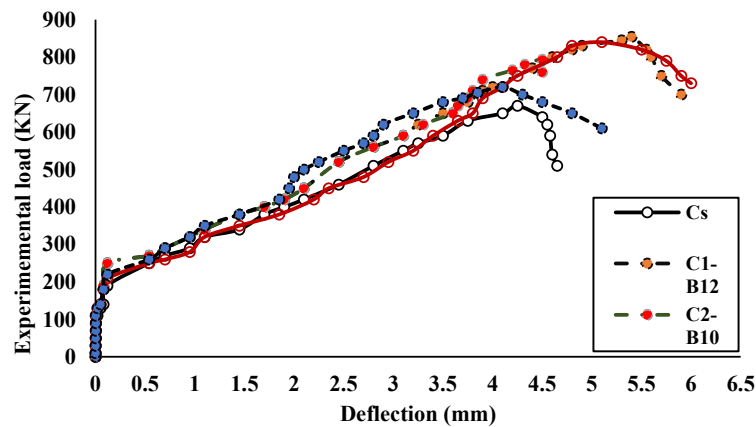
Fig. 3: Comparison between experimental failure load (kN).

	Cs	C1-B12	C2-B10	C3-B12	C4-B10
EXP	669	854	793	840	720
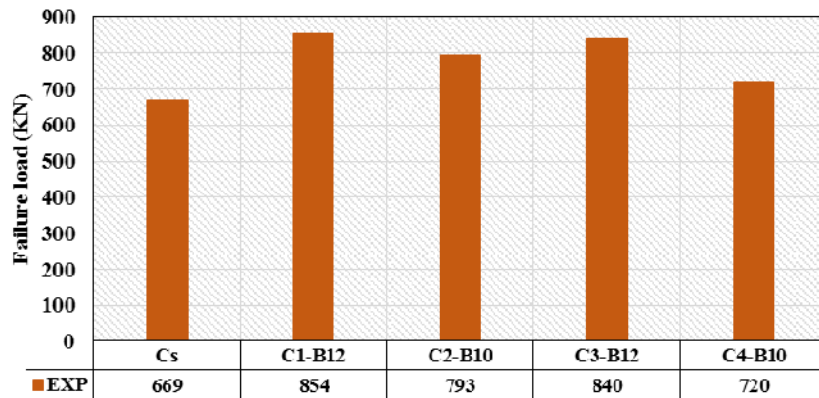
Fig. 4: Experimental failure load (kN) for different columns

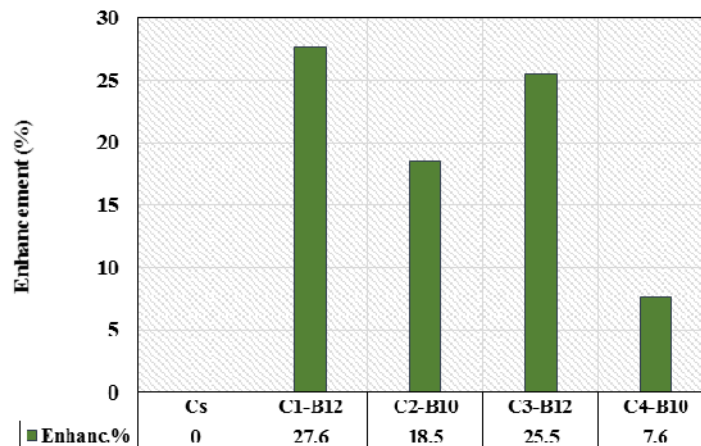|	Cs	C1-B12	C2-B10	C3-B12	C4-B10
Enhanc.%	0	27.6	18.5	25.5	7.6

Fig. 5: Comparasion between percentage of experimental failure load enhancement.

3.2 Experimental cracks of concrete columns

The cracks for concrete columns will be discussed. The initiation of cracks in column Cs was unseen but the first seen one was at load of 250kN at the column head under the point of load concentration. The cracks propagated till reach the maximum load of 669.0kN. Then, load decrease in load take place and the cracks propagated and increased showing failure of column. This propagation in cracks is normal in columns due to the distance between column stirrups as shown in Fig. 6.

For columns specimens which reinforced using basalt bars only C_{1-B12} and C_{2-B10}, the first crack appears at lateral stage due to its tensile strength which were at 370.0 KN and 320KN.
For the specimens use basalt bars and stirrups with less number and large spacing between stirrups C_{3-B12} and C_{4-B10}, the first crack also delayed to be at 350.0KN and 290.0KN.
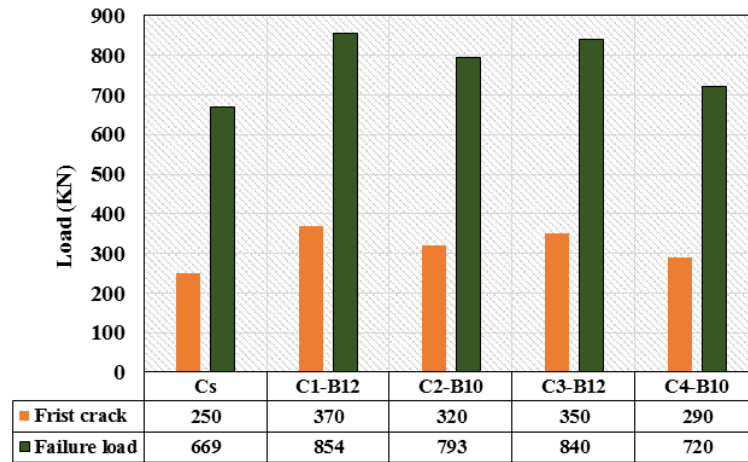This due to the high efficiency of stirrups tensile strength. The experimental crack pattern is indicated in Fig. 7.

	Cs	C1-B12	C2-B10	C3-B12	C4-B10
■ Frist crack	250	370	320	350	290
■ Failure load	669	854	793	840	720

Fig. 6: Comparison between first crack loads and Max. Load for different columns

3.3 Mode of Failure

The concrete column Cs failed in a mode of compression failure accompanied with local crushing and spalling of the concrete cover and at the head under the point of applied load. For the other concrete columns reinforced using BFRP bars, near failure the load reach the maximum value and after this value the load decreased up to 70% to 50% of the maximum load with increasing the descending part of load displacement curves. This increases of descending part represent type of ductility and safe line in using the structures as shown in Fig. 3. The failure of the concrete columns reinforced by basalt bars take mode of brittle failure especially after reaching the allowable value of tensile strength of bars and stirrups which increase the confinement of column, leading to increase of ultimate load.
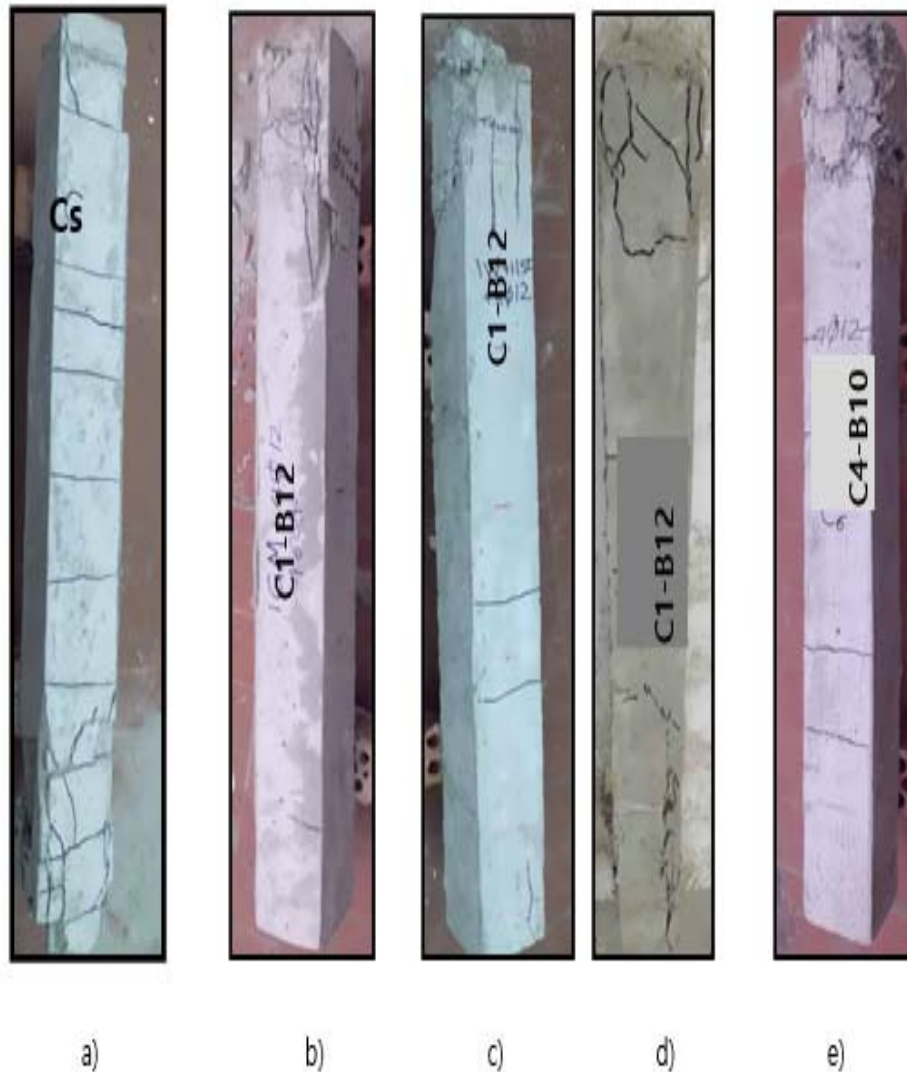
Fig. 7: Cracking pattern; a) Cs; b) C_{1-B12}; c) C_{2-B10}; d) C_{3-B12}; e) C_{4-B10}

3.4 Ductility and Energy Absorption of Tested Columns

The calculated ratio between the deformations at 0.8 of ultimate load in the descending part to the deformation at the ultimate load is the ductility, but the energy absorption of the specimen is the total area under the load deflection curve.

Ductility obtained from the experimental test was shown in Fig. 8 and Table 3 discussed as the following. The ductility obtained for the control specimen Cs was 1.15 but a progressive increase in ductility obtained for different specimens.

For columns reinforced using BFRP bars, the ductility varied between 1.13 to 1.07 with a decrease in ductility varied between 1.73% to 7.0%. This decrease may be due to the behaviour of basalt bars failure.

Fig. 9 shows the energy absorption for the tested columns. The progressive increase of energy absorption was observed while for the specimen Cs the energy absorption recorded 1591.0 KN.mm. By comparing this value with the recorded for different columns it shows good enhancement. It can be state that it delayed the appearance of the first cracks and increased the service load capacity.

The calculated energy absorption for C_{1-B12}, C_{2-B10}, C_{3-B12} and C_{4-B10} were 2239.0KN.mm, 1784.0KN.mm, 2142.0KN.mm and 1476.0KN.mm respectively. It developed with high ultimate loads, crack resistance, high durability, high ductility and energy absorption properties, which are very useful for dynamic applications.
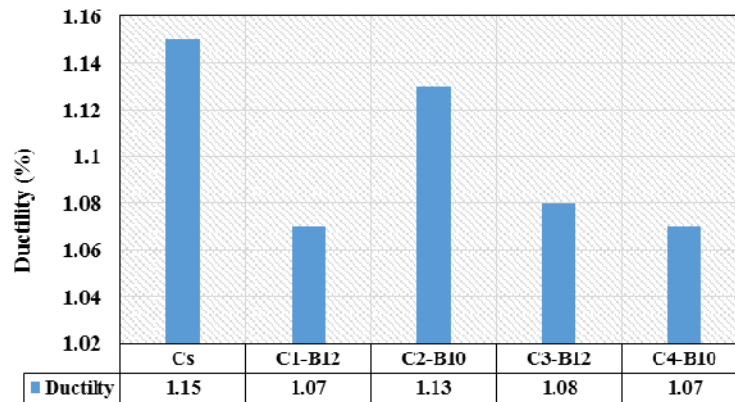
	Cs	C1-B12	C2-B10	C3-B12	C4-B10
■ Ductilty	1.15	1.07	1.13	1.08	1.07

Fig. 8: Comparisons between the obtained ductility for tested specimens

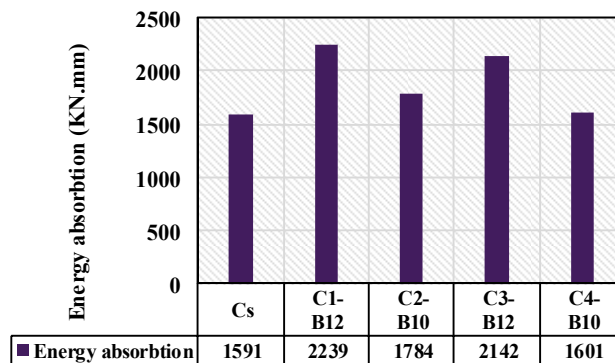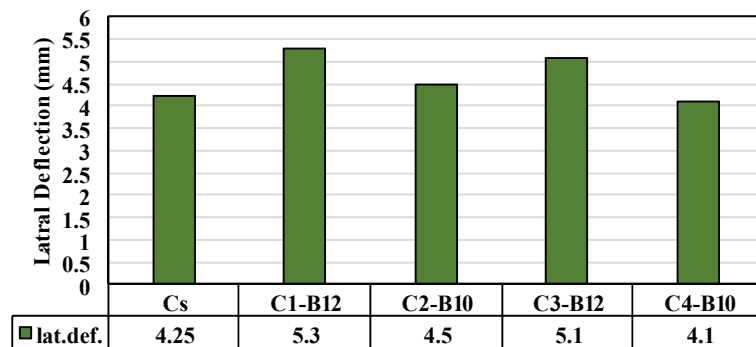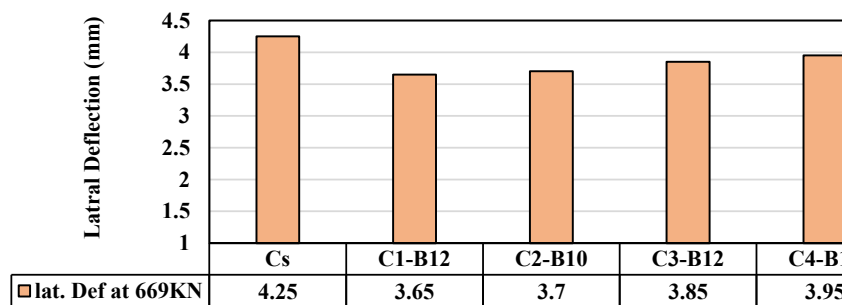|	Cs	C1-B12	C2-B10	C3-B12	C4-B10
■ Energy absorbtion	1591	2239	1784	2142	1601

Fig. 9: Comparisons between the energy absorption for tested specimens

3.5 Lateral Deformation for concrete columns

For columns which examined, the lateral displacement is the most affected in the column. So, column in this case of using reinforcing steel recorded the maximum values of lateral displacement to be 4.25mm at load of 669.0KN which is the failure load of specimen Cs as given in Table 4. For the column specimens reinforcing using BFRP bar especially 4 Φ 12 the lateral deformation enhanced to be 3.65mm at load of 669.0KN but at its failure load it recorded 5.3 mm. for specimen C_{2-B10} the maximum lateral displacement at failure load was 4.5 mm but at failure load of Cs it was 3.70mm. it may be explained due to good confinement of basalt stirrups while it had high tensile strength. For the specimens C_{3-B12} and C_{4-B10} the lateral displacements were 5.1mm and 4.1mm compered to be 3.85mm and 3.95mm respectively at load of 669.0KN for the control column. This relative increase in lateral displacement due to decreasing number of basalt stirrups and increasing the space between them which effect on confinement. Finally, due to prefect confinement happened due to the usage of Basalt stirrups enhanced the behavior of the tested columns. It can be state that it delayed the appearance of cracks and increased the load capacity. Also, it enhanced the lateral deflection as shown in Fig. 10.

	Cs	C1-B12	C2-B10	C3-B12	C4-B10
lat.def.	4.25	5.3	4.5	5.1	4.1

a)

	Cs	C1-B12	C2-B10	C3-B12	C4-B1
lat. Def at 669KN	4.25	3.65	3.7	3.85	3.95

b)

Fig. 10: Comparisons between lateral deflections for tested columns, a) lateral deformation at max. Load; b) lateral deformation at max. Load of Cs

4. Non-Linear Finite Element Analysis (NLFEA)

NLFEA was carried out to investigate the behaviour of the HSC concrete columns reinforced by basalt FRP using ANSYS-14.5 computer program [45]. The study contains the pattern of cracks, the ultimate failure load and the load-deflection curves.

4.1. Reinforced Concrete Columns Modelling

3-D modelling was conducted for HSC columns reinforced by BFRP bars using ANSYS-14.5. Element solid65 was used for representing the concrete columns and element link10 was used for representing reinforcing steel & basalt bars as in Fig. 11.
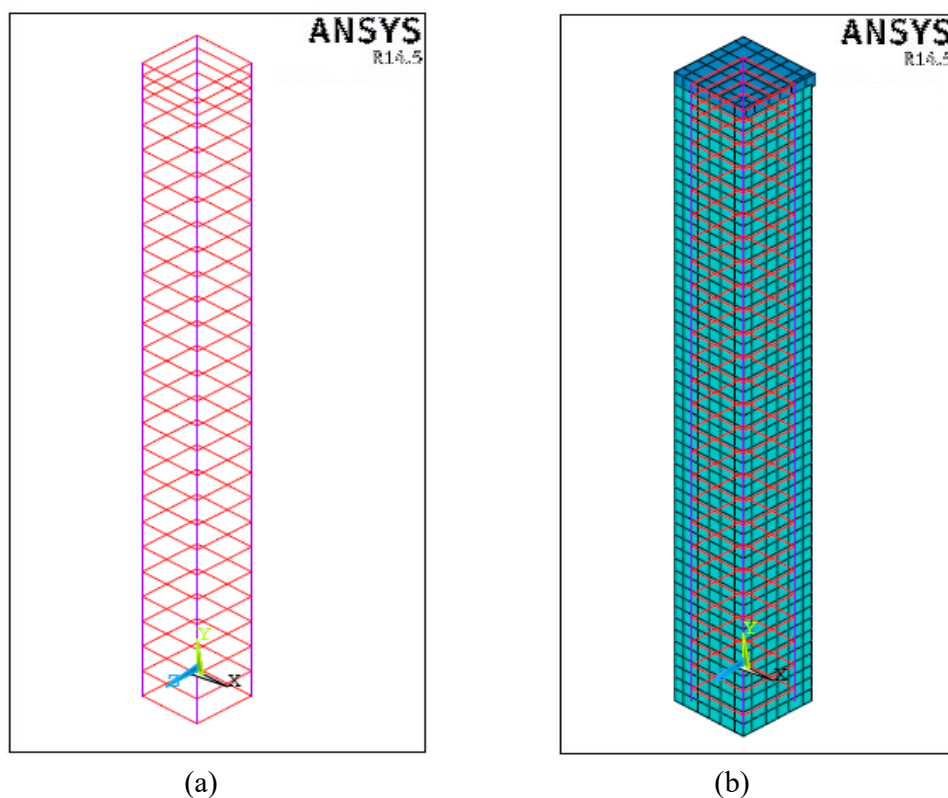

(a)   (b)

Fig.11: Analytical Model, a) link10 for bars, b) solid65 for concrete.

4.2 NLFE ultimate loading carrying capacity

Table 4 shows the ultimate failure loads of all columns. The ultimate failure load of control column Cs is 603 KN. The columns from C_{1-B12} to C_{4-B10} had relatively higher ultimate failure loads than control which ranged from 630kN to 718kN.

The analytical enhancement in ultimate load capacity p_u was recorded by specimens C_{1-B12}, C_{2-B10}, C_{3-B12} and C_{4-B10} with enhancement of 19.1 %, 5.14%, 4.48% and 6.10% respectively.

4.3 NLFE lateral deformation

Table 4 shows the lateral displacement of all columns. The lateral displacement for Cs was 3.80 mm for the reference specimen. For C_{2-B10}, C_{3-B12} and C_{4-B10} the lateral displacement was 4.50 mm, 3.60 mm and 3.85 mm respectively.

Using the basalt stirrups instead of steel stirrups increased the confinement of the columns, ductility and analytical failure load as in Table 4. So, using basalt bars generally enhanced the behavior of the analytical columns.

5. Comparison between experimental and finite element analysis results

The objective of the comparison of experimental and finite element results is to confirm that analytical 3D models are meet to represent the behavior response of the HSC basalt FRP columns. The five analytical 3D models were compared with the experimental results in expressions of ultimate load, ultimate deflection, and crack pattern.

This is compatible with Tu et al. [46]. They showed that decreasing the stirrup spacing might avoid the failure of buckling for the longitudinal bars and enhanced the ductility and failure ultimate load of the GFRP-RC columns.

5.1 Ultimate failure load

Fig. 12 showed a good acceptable agreement between the experimental & NLFEA ultimate failure load capacity Pu $_{NLFEA}$/Pu $_{exp.}$. Also, Fig. 14 presented compatibility between the analytical & experimental studied. Referring to Table 4, Pu $_{NLFEA}$/Pu $_{exp}$ ratio for control specimen column Cs was 0.90. While ratios were 0.84, 0.86, 0.75 and 0.89 for C_{1-B12}, C_{2-B10}, C_{3-B12} and C_{4-B10} respectively. The average agreement for all specimens is equals to 0.85 which reflected the effect of using finite element analysis.

5.2. Ultimate lateral deflection

Fig. 12 showed an acceptable agreement between the experimental & NLFEA ultimate failure load capacity Δu $_{NLFEA}$ / Δu $_{exp..}$ Figure 12 showed comparison between experimental lateral deflection and NLFEA one. Figure 14 showed the load deflection curves for all columns in both experimental and analytical manners. The load displacement curves for tested specimens and analytical results showed a good acceptable agreement. Referring to Table 4, Δu $_{NLFEA}$ / Δu $_{exp.}$ of the control specimen column Cs was 0.89. While ratios were 0.85, 0.80, 0.75 and 0.89 for C_{1-B12}, C_{2-B10}, C_{3-B12} and C_{4-B10} respectively. The average agreement for all specimens is equals to 0.85 which reflected the effect of using finite element analysis.
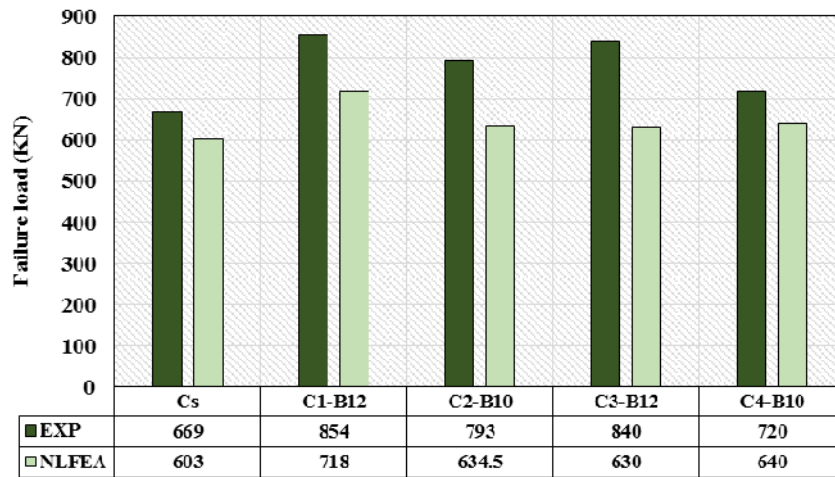
	Cs	C1-B12	C2-B10	C3-B12	C4-B10
■ EXP	669	854	793	840	720
□ NLFEA	603	718	634.5	630	640

Fig. 12 Comparison between experimental and analytical failure load

|	Cs	C1-B12	C2-B10	C3-B12	C4-B10
■ EXP	4.25	5.3	4.5	5.1	4.1
□ NLFEA	3.8	4.5	3.6	3.85	3.65
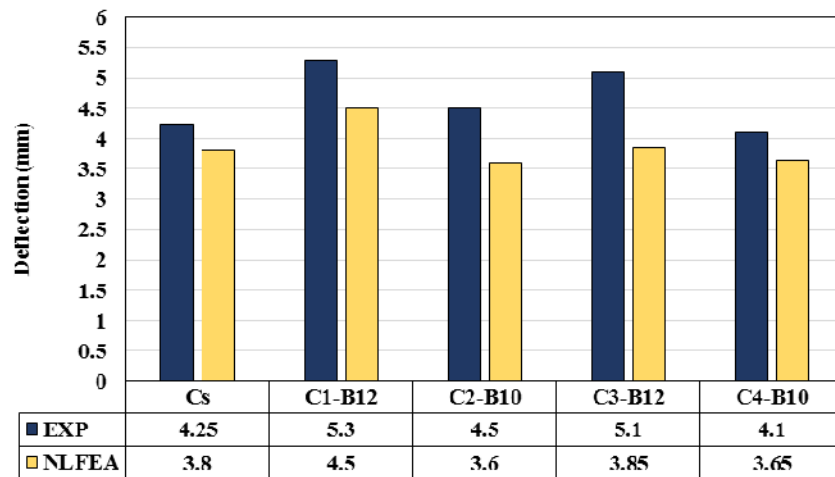
Fig. 13 Comparison between experimental and analytical lateral deflection

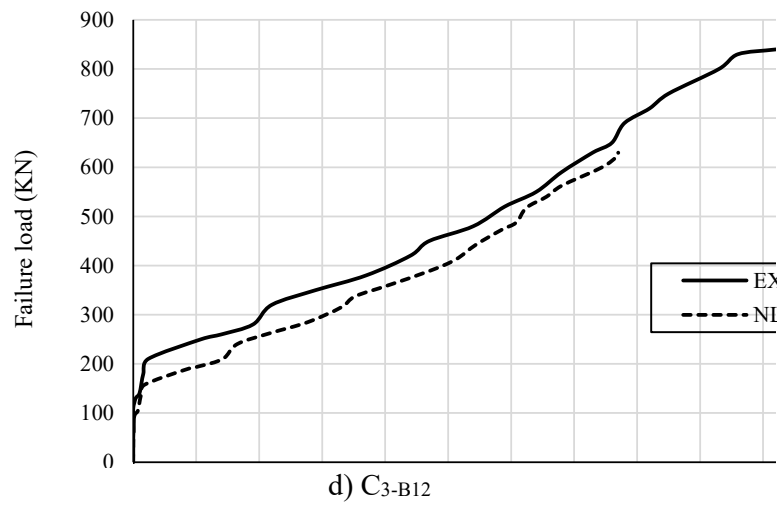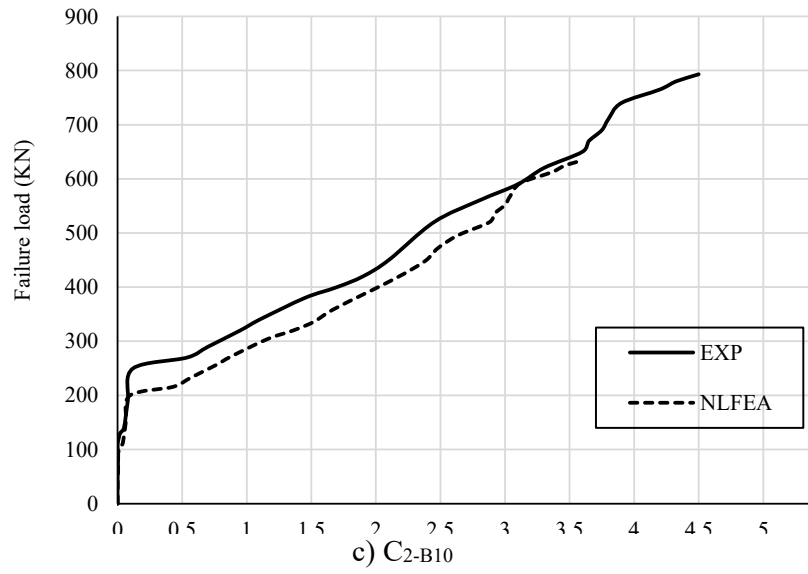Table:4 Comparisons between experimental and finite element results

Specimen Id	Reinforcement	Failure Load P_{Umax} (kN)		P_{Umax} Agreement (%)	Lateral Displacement Δ_{Umax} (mm)		Δ_{Umax} Agreement (%)
		EXP.	NLFE	NLFE/EXP.	EXP.	NLFE	NLFE/EXP.
Cs	4Φ12+15Φ8 stirrups	669.0	603.0	90.0	4.25	3.80	89.0
C_{1-B12}	4Φ12 BFRP+15Φ8 steel stirrups	854.0	718.0	84.0	5.30	4.50	85.0
C_{2-B10}	4Φ10 BFRP+15Φ8 steel stirrups	739.0	634.0	86.0	4.50	3.60	80.0
C_{3-B12}	4Φ12 BFRP+10Φ8 basalt stirrups	840.0	630.0	75.0	5.10	3.85	75.0
C_{4-B10}	4Φ12+10 Φ8 basalt stirrups	720.0	640.0	89.0	4.10	3.65	89.0

a) Cs

b) C_{1-B12}

c) C$_{2\text{-B10}}$

d) C$_{3\text{-B12}}$
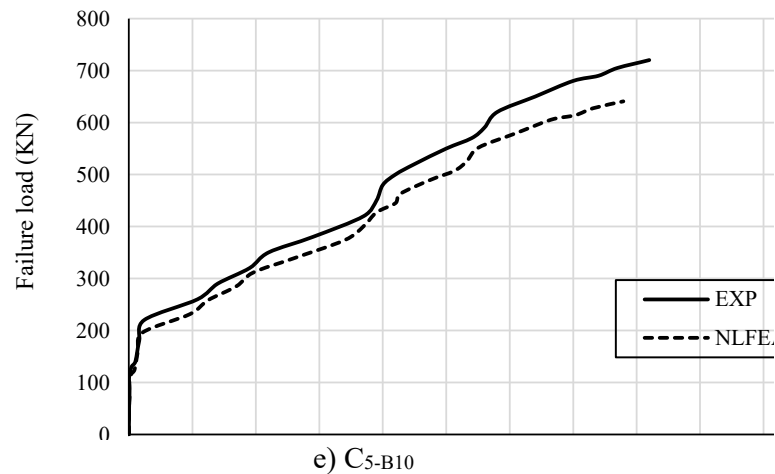
e) $C_{5\text{-}B10}$
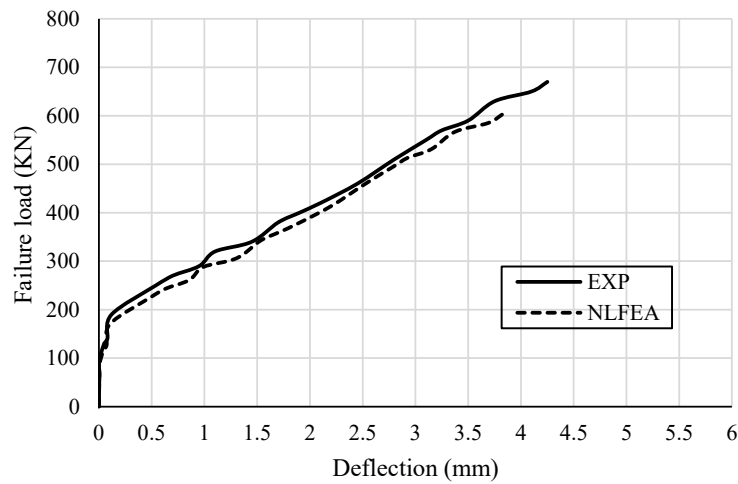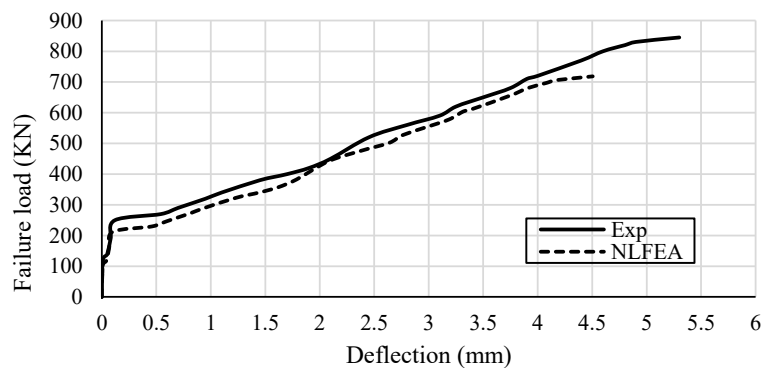
Fig. 14 Comparison between EXP. and NLFEA load displacement curves for columns

5.2. Ultimate lateral deflection

Fig. 12 showed a good acceptable agreement between the experimental & NLFEA ultimate failure load capacity $\Delta u_{NLFEA} / \Delta u_{exp..}$ Fig. 12 showed comparison between experimental lateral deflection and NLFEA one. Fig. 14 displayed the experimental & analytical load-deflection curves for all columns. The load displacement curves for tested specimens and analytical results showed a good acceptable agreement. Referring to Table 4, $\Delta u_{NLFEA} / \Delta u_{exp.}$ of the control specimen column Cs was 0.89. While ratios were 0.85, 0.80, 0.75 and 0.89 for $C_{1\text{-}B12}$, $C_{2\text{-}B10}$, $C_{3\text{-}B12}$ and $C_{4\text{-}B10}$ respectively. The average agreement for all specimens is equals to 0.85 which reflected the effect of using finite element analysis.

5.3. Pattern of cracks

The crack patterns obtained from experimental work and non-linear finite element analysis for all columns presented an approximately similar patterns of crack propagation in compression failure. Fig.15 specify control specimen column Cs. These cracks are horizontal flexural tension crack at column edges and transverse vertical cracks that happened in concrete crushing. The analytical model of crack propagation is in good acceptable agreement with experimental one.
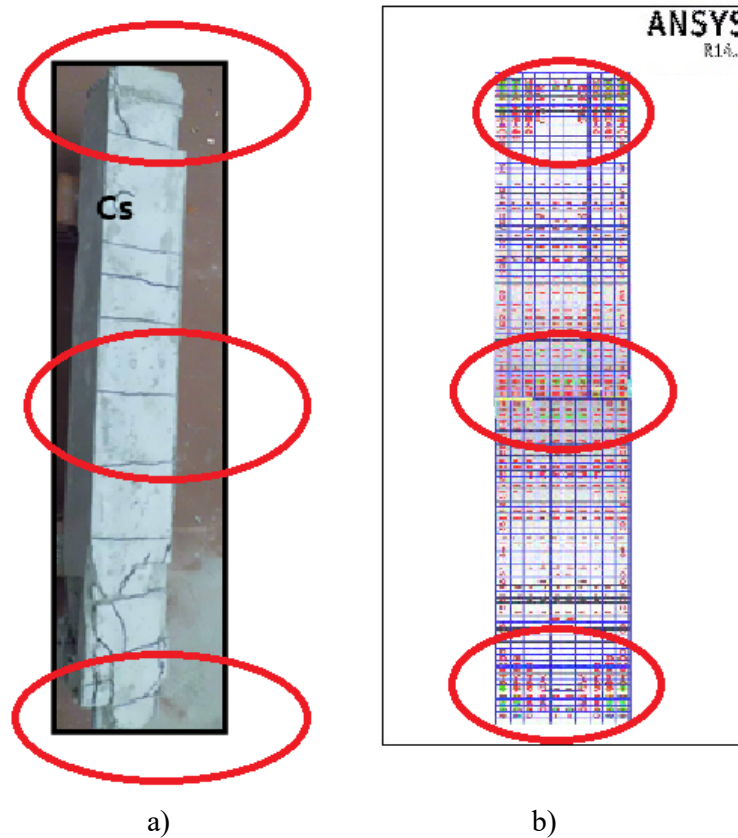
a)   b)
Fig. 15 Pattern of cracks for examined control column Cs

6. Conclusions

Based on the obtained results and observations of the experimental and the analytical study presented in this research paper and considering the relatively high variability and the statistical pattern of data, the following conclusions can be drawn:

- Using the reinforcing steel bars as column reinforcement has effect in the column carrying capacity, especially in case of using steel stirrups which increase the confinement leading to increase the carrying capacity.

- Basalt FRP bars have high tensile strength relative to steel bars. This led to increasing the carrying load capacity of concrete columns at small bars diameters.

- Using BFRP stirrups increase the confinement of concrete, which decrease the lateral displacement, cracks numbers, crack width and increasing the column capacity.

- Experimental results revealed that using Basalt FRP bars as reinforcement contributed to higher ultimate load, ductility and higher energy absorption.

- When comparing the obtained lateral deflection for column Cs with the other which used the BFRP bars or stirrups have a great effect in enhancing, the deflection showing good confinement and improvement in ductility and energy absorption.

- There is a good acceptable agreement between experimental & analytical one. This might be recognized that wisely under taken experimental study was done and might be supportive for future parametric studies.

References

[1] Focacci F, Nanni A, Bakis CE. Local bond–slip relationship for FRP reinforcement in concrete. ASCE J Compos Constr 2000;4(1):24–31.
[2] Haroun MA, Elsanadedy HM. Behavior of cyclically loaded squat reinforced concrete bridge columns upgraded with advanced composite-material jackets. J Bridge Eng 2005;10(6):741–8. [3] Niu H, Wu Z. Numerical analysis of debonding mechanisms in FRPstrengthened RC beams. Comput-Aided Civ Infrastruct Eng 2005;20 (5):354–68.
[4] Fahmy MFM, Wu ZS, Wu G. Post-earthquake recoverability of existing RC bridge piers retrofitted with FRP composites. J Constr Building Mater 2010;24 (6):980–98.
[5] Choi E, Jeon J, Cho B, Park K. External jacket of FRP wire for confining concrete and its advantages. J. Eng Struct 2013; 56:555–66.
[6] Zhao J, Sritharan S. Modeling of strain penetration effects in fiber-based analysis of reinforced concrete structures. ACI Struct J 2007;104(2):133–41.
[7] Murcia-Delso J, Stavridis A, Shing B. Modeling the bond–slip behavior of confined large diameter reinforcing bars. In: III ECCOMAS thematic conference on computational methods in structural dynamics and earthquake engineering; 2011.
[8] Tighiouart B, Benmokrane B, Gao D. Investigation of bond in concrete member with fiber reinforced polymer (FRP) bars. Constr Building Mater 1998;8 (12):453–62.
[9] Fahmy MFM, Wu Z. Bond-based earthquake-proof of RC bridge columns reinforced with steel rebars and SFCBs. Earthquake-resistant structures – design, assessment and rehabilitation 2011; 2012. p. 429–54.
[10] E. Adda-Bedia, W.S. Han, G. Verchery, Simplified methods for prediction of moisture diffusion in polymer matrix composites with cyclic environmental conditions, Polym. Polym. Compos. 6 (04) (1998) 189–203.
[11] Z.Z. Li, A.M. Yu, Y.L. Wang, Durability of FRP rebars in alkaline environment of concrete, Build. Sci. 29 (01) (2013) 47–51.
[12] B. Benmokrane, F. Elgabbas, E.A. Ahmed, P. Cousin, Characterization and comparative durability study of glass/vinylester, basalt/vinylester, and basalt/ epoxy FRP bars, J. Compos. Constr. 19 (06) (2015). 04015008-1-04015008-6.

[13] El Refai A, Ammar M, Masmoudi R. Bond performance of basalt fiberreinforced polymer bars to concrete". J Compos Constr 2015;19(3):04014050.

[14] Ibrahim AMA, Wu Z, Fahmy MFM, Kamal D. Experimental study on cyclic response of concrete bridge columns reinforced by steel and basalt FRP reinforcements. ASCE J Compos Constr 2015. CC.1943-5614.0000614, 04015062.

[15] Ibrahim AMA, Fahmy MFM, Wu Z. Numerical simulation on fracturing bond mechanisms of different basalt FRP bars. JSCE J Applied Mechanics 2015;71(2):I_289–98.

[16] Eligehausen R, Popov EP, Bertero VV. Local bond stress-slip relationships of deformed bars under generalized excitations. Report No. UCB/EERC-83/23, Berkeley, California, USA: University of California; 1983.

[17] S. Amidi, J. Wang, Subcritical debonding of FRP-to-concrete bonded interface under synergistic effect of load, moisture, and temperature, Mech. Mater. 92 (2016) 80–93.

[18] A. El Refai, M.-A. Ammar, R. Masmoudi, Bond performance of basalt fiberreinforced polymer bars to concrete, J. Compos. Constr. 19 (3) (2014) 04014050.

[19] A. El-Nemr, E.A. Ahmed, C. Barris, B. Benmokrane, Bond-dependent coefficient of glass- and carbon-FRP bars in normal- and high-strength concretes, Constr. Build. Mater. 113 (2016) 77–89.

[20] Z. Dong, G. Wu, Y. Xu, Experimental study on the bond durability between steel-FRP composite bars (SFCBs) and sea sand concrete in ocean environment, Constr. Build. Mater. 115 (2016) 277–284.

[21] R. Goyal, A. Mukherjee, S. Goyal, An investigation on bond between FRP stayin- place formwork and concrete, Constr. Build. Mater. 113 (2016) 741–751.

[22] H. Fang, X. Xu, W. Liu, Y. Qi, Y. Bai, B. Zhang, D. Hui, Flexural behavior of composite concrete slabs reinforced by FRP grid facesheets, Composites Part B 92 (2016) 46–62.

[23] A. Yazdanbakhsh, L.C. Bank, The effect of shear strength on load capacity of FRP strengthened beams with recycled concrete aggregateconcrete, Constr. Build. Mater. 102 (Part 1) (2016) 133–140.

[24] L. Zhang, Y. Sun, W. Xiong, Experimental study on the flexural deflections of concrete beam reinforced with Basalt FRP bars, Mater. Struct. 48 (10) (2015) 3279–3293.

[25] T.H.-K. Kang, M.I. Ary, Shear-strengthening of reinforced & Prestressed concrete beams using FRP: Part II - Experimental Investigation, Int. J. Concr. Struct. Mater. 6 (1) (2012) 49–57. [26] M. Corradi, L. Righetti, A. Borri, Bond strength of composite CFRP reinforcing bars in timber, Materials 8 (7) (2015) 4034.

[27] A. Shukri, K. Darain, M. Jumaat, The tension-stiffening contribution of NSM CFRP to the behavior of strengthened RC beams, Materials 8 (7) (2015) 4131.

[28] G. Nossoni, R.S. Harichandran, M.I. Baiyasi, Rate of reinforcement corrosion and stress concentration in concrete columns repaired with bonded and unbonded FRP wraps, J. Compos. Constr. 19 (5) (2015).

[29] O. Youssf, M.A. ElGawady, J.E. Mills, Displacement and plastic hinge length of FRP-confined circular reinforced concrete columns, Eng. Struct. 101 (2015) 465–476.

[30] P. Yin, L. Huang, L. Yan, D. Zhu, Compressive behavior of concrete confined by CFRP and transverse spiral reinforcement. Part A: experimental study, Mater. Struct. 49 (3) (2016)

1001–1011.

[31] R. Abbasnia, H. Ziaadiny, Experimental investigation and strength modeling of CFRP-confined concrete rectangular prisms under axial monotonic compression, Mater. Struct. 48 (1–2) (2015) 485–500.

[32] M.N. Hadi, Q.S. Khan, M.N. Sheikh, Axial and flexural behavior of unreinforced and FRP bar reinforced circular concrete filled FRP tube columns, Constr. Build. Mater. 122 (2016) 43–53.

[33] Shi J, Zhu H, Wu Z, Wu G. Durability of BFRP and hybrid FRP sheets under freeze-thaw cycling. Adv Mater Res 2011;163e167:3297e300.

[34] Liu H, Lu Z, Peng Z. Test research on prestressed beam of inorganic polymer concrete. Mater Struct 2015; 48:1919e30.

[35] Wei B, Cao H, Song S. Environmental resistance and mechanical performance of basalt and glass fibers. Mater Sci Eng A 2010;527(18e19):4708e15.

[36] Lee JJ, Song J, Kim H. Chemical stability of basalt fiber in alkaline solution. Fibres Polym 2014;15(11):2329e34.

[37] Li W, Xu J. Mechanical properties of basalt fiber reinforced geopolymeric concrete under impact loading. Mater Sci Eng A 2009; 505:178e86.

[38] Wu G, Dong Z, Wang X, Zhu Y, Wu Z. Prediction of long-term performance and durability of BFRP bars under the combined effect of sustained load and corrosive solutions. J Compos Constr 2015;19(3):04014058.

[39] Tomlinson D, Fam A. Performance of concrete beams reinforced with basalt FRP for flexure and shear. J Compos Constr 2015;19(2):04014036.

[40] Zhang L, Sun Y, Xiong W. Experimental study on the flexural deflections of concrete beam reinforced with Basalt FRP bars. Mater Struct 2015;48: 3279e93.

[41] Ge W, Zhang J, Cao D. Tu. Flexural behaviors of hybrid concrete beams reinforced with BFRP bars and steel bars. Constr Build Mater 2015; 87:28e37.

[42] A. EI Refai, F. Abed. Concrete contribution to shear strength of beams reinforced with basalt fiber-reinforced bars. J Compos Constr 10.1061/(ASCE) CC.1943-5614.0000648, 04015082.

[43] Erfan Abeer M.; Algash Yasser A.; and El-Sayed, Taha A. Experimental & Analytical Flexural Behavior of Concrete Beams Reinforced with Basalt Fiber Reinforced Polymers Bars. International Journal of Scientific and Engineering Research 2019, 10(8), 297–315.

[44] El-Sayed, Taha A., Flexural behavior of RC beams containing recycled industrial wastes as steel fibers. Construction and Building Materials 212, (2019): 27-38.

[45] ANSYS," Engineering Analysis system user's Manual" 2014, vol. 1&2, and theoretical manual. Revision 14.5, Swanson analysis system inc., Houston, Pennsylvania.

[46] Tu J, Gao K, He L, Li X. Experimental study on the axial compression performance of GFRP-reinforced concrete square columns. Advances in Structural Engineering. 2019 May;22(7):1554-65.